

# Variability in the durability of CRISPR-Cas immunity

Hélène Chabas<sup>1</sup>, Antoine Nicot<sup>1</sup>, Sean Meaden<sup>2</sup>, Edze Westra<sup>2</sup>, Denise Tremblay<sup>3,4</sup>, Léa Pradier<sup>1</sup>, Sébastien Lion<sup>1</sup>, Sylvain Moineau<sup>3,4</sup> and Sylvain Gandon<sup>1</sup>

<sup>1</sup>CEFE UMR 5175, CNRS – Université de Montpellier – Université Paul-Valéry Montpellier – EPHE, 1919, route de Mende, 34293 Montpellier Cedex 5, France

<sup>2</sup>Environment and Sustainability Institute, University of Exeter, Penryn Campus, Penryn, Cornwall, TR10 9FE, UK

<sup>3</sup>Département de biochimie, microbiologie et de bio-informatique, Faculté des sciences et de génie, Université Laval, 1045 avenue de la Médecine, Québec City, QC, Canada, G1V 0A6

<sup>4</sup>Félix d'Hérelle Reference Center for Bacterial Viruses and Groupe de recherche en écologie buccale, Faculté de médecine dentaire, Université Laval, Québec City, QC, Canada, G1V 0A6

**Keywords:** Durability of resistance, pathogen evolution, CRISPR-Cas, mutation rates

## Abstract

The durability of host resistance is challenged by the ability of pathogens to escape the defense systems of their hosts. Understanding the variability in the durability of host resistance is of paramount importance for designing more effective control strategies against infectious diseases. Here we study the durability of various CRISPR-Cas alleles of the bacteria *Streptococcus thermophilus* against lytic phages. We found substantial variability in durability among different resistant bacteria. Since the escape of the phage is driven by a mutation in the phage sequence targeted by CRISPR-Cas, we explored the fitness costs associated with these escape mutations. We found that, on average, escape mutations decrease the fitness of the phage. Yet, the magnitude of this fitness cost does not predict the durability of CRISPR-Cas immunity. We contend that this variability in the durability of resistance may be due to variations in phage mutation rate or in the proportion of lethal mutations across the phage genome. These results have important implications for the understanding of the coevolution between bacteria and phages and for the optimal deployment of resistance strategies against pathogens and pests. In a broader perspective, understanding the durability of CRISPR-Cas immunity may also help develop more effective gene-drive strategies based on CRISPR-Cas9 technology.

## 33 Introduction

34 Public health and agriculture are constantly challenged by the spread of infectious diseases.  
35 An arsenal of various prophylactic and therapeutic strategies has been developed to limit  
36 the circulation of pathogens (e.g. introgression of resistance genes in plant varieties, use of  
37 antimicrobial drugs). Yet, the efficacy of those interventions can be rapidly eroded by the  
38 evolution of pathogen populations [1, 2, 3, 4]. It is important to note that distinct defense  
39 strategies may lead to very different evolutionary outcomes. For instance, imperfect  
40 immunity is known to select for more aggressiveness and virulence in pathogens [5, 6].  
41 In addition, distinct defense strategies may differ in their level of *durability*. Why are  
42 some host defense strategies overcome very rapidly while others remain effective for a  
43 long period of time [4, 7, 8]? A better understanding of the durability of host defenses  
44 (defined as the inverse of the speed of pathogen adaptation to those defenses) is key for  
45 the development of sustainable management strategies of pathogens and pests [7, 9].

46  
47 Empirical and experimental studies in plant pathosystems have played key roles in the  
48 identification of major factors acting on the durability of host resistance [4, 7, 9, 10, 11].  
49 For instance, the type of plant resistance is known to have a significant impact on the  
50 speed of pathogen adaptation. *Qualitative* resistance, an all-or-nothing response, is often  
51 considered to be less durable than *quantitative* resistance, which reduces disease progres-  
52 sion in the plant. This effect is usually attributed to the simpler genetic determinism  
53 of pathogen adaptation to qualitative resistance which involves a few (or even a single)  
54 major virulence genes [12]. In contrast, adaptation to the polygenic determinism of  
55 quantitative resistance requires multiple pathogen mutations [13, 14]. Yet, qualitative  
56 resistance exhibits much variation in durability [4]. A classical explanation for this  
57 variation in durability involves selective constraints acting on the pathogen population.  
58 More specifically, host defense is likely to be more durable if the mutations (virulence  
59 alleles) that allow the pathogen to escape qualitative resistance are associated with fitness  
60 costs [4, 12]. Understanding the selective constraints acting on the sites targeted by  
61 different resistance mechanisms may help predict the durability of resistance and limit the  
62 speed of pathogen adaptation [4, 15]. Testing this hypothesis, however, is often difficult  
63 in plant pathosystems where measuring the durability of specific resistance mechanisms  
64 in controlled experiments raises practical difficulties [16, 17].

65

66 Here we use the interaction between bacteria and their lytic bacteriophages (or phages)  
67 to study the factors that modulate the durability of host resistance. Bacteria have access  
68 to a wide range of defense systems to defend themselves against phages [18, 19, 20, 21].  
69 Among these distinct defense systems, CRISPR–Cas (Clustered Regularly Interspaced  
70 Short Palindromic Repeats – CRISPR Associated Genes) has the unique ability to  
71 generate hundreds of different alleles of resistance targeting different sites in the phage  
72 genome [22]. Here, we exploit this unique property to explore the variability in durability  
73 among distinct CRISPR–Cas resistance alleles targeting the same phage. CRISPR-Cas  
74 is an adaptive prokaryotic immune defense which integrates into the CRISPR locus  
75 (integration of a spacer) a small phage-DNA sequence (the protospacer, here 30 bp  
76 long) from an invading genome and uses this memory to target and degrade subsequent  
77 invading matching DNA (interference) [23]. To select and integrate a specific protospacer  
78 from a foreign nucleic acid into its CRISPR array, many CRISPR–Cas systems rely on  
79 a 2-5 bp sequence, the PAM (Protospacer Adjacent Motif) [24], flanking one side of  
80 the protospacer sequence and mandatory for spacer integration and interference. Given  
81 its size, the PAM is present numerous times on the phage genome, leading potentially  
82 to hundreds of different resistances targeting various protospacers [22]. In this system,  
83 phages can only escape CRISPR-Cas by mutating their PAM or seed sequence (ie. the  
84 proximal part of the protospacer) [25]. As such, CRISPR-Cas immunity corresponds to  
85 a very specific form of *qualitative* resistance. In the following, we first quantified the  
86 ability of a phage to escape a set of resistant bacteria, each of them having a distinct  
87 new spacer targeting a unique single protospacer site in the phage genome. Second, we  
88 isolated escape phage mutants on each of the resistant bacteria (e.g. each phage escape is  
89 mutated at a specific and different protospacer region) and we characterized their relative  
90 fitness during the infection of a population of phage-sensitive bacteria. This experimental  
91 protocol allowed us to discuss the potential link between the fitness effects of escape  
92 mutations in the phage and the durability of different resistance alleles in the bacteria.

## 93 **Materials and Methods**

### 94 **Bacterial strains and phages**

95 The **clonal** bacterium *Streptococcus thermophilus* DGCC 7710 (WT) and its **clonal** virulent  
96 phage 2972 were obtained from the Félix d’Hérelle Reference Center for Bacterial Viruses  
97 ([www.phage.ulaval.ca](http://www.phage.ulaval.ca)) [26]. Bacteria were grown in LM17 broth (M17 Oxoid (37 g/L  
98 with 5g/L of lactose) and incubated at 40°C. For phage amplification 10 mM of sterile  
99 CaCl<sub>2</sub> were added to the broth. Using a standardized protocol described in [27], a culture

100 of *S. thermophilus* DGCC 7710 was challenged with the virulent phage 2972, and the  
101 surviving colonies/cells (BIMs, Bacteriophage Insensitive Mutants) were screened by PCR  
102 for expansion of their CRISPR array, followed by a 2% agarose electrophoresis. Primer  
103 sequences and PCR protocol can be found in supplementary information A. We confirmed  
104 that each BIM possesses a different spacer by Sanger sequencing the newly acquired  
105 spacer (Eurofins Genomics). A total of 17 different BIMs, each with a single and distinct  
106 spacer acquired into the active CRISPR1 locus of a type II-A CRISPR-Cas system,  
107 were kept and used in this study. Spacer sequences are provided in the supplementary  
108 information B. Finally, protospacers were positioned on the genome of phage 2972 that  
109 is published in [26].

### 110 **Phage detection and titration**

111 Bacterial lawns were produced by plating 6 mL of soft agar (LM17+CaCl<sub>2</sub> with 0.8%  
112 agar and 400  $\mu$ L of bacteria in mid-exponential phase) on top of plates previously poured  
113 with 30 mL of hard agar (LM17+CaCl<sub>2</sub> with 1.5% agar). For phage titration, 50  $\mu$ L of  
114 diluted phages were added to soft agar. For phage detection, 5  $\mu$ L of phage solution were  
115 spotted directly on the solidified soft agar. When needed, phages were diluted in phage  
116 buffer (50 mM Tris-HCl pH7.5 + 100 mM NaCl + 8 mM MgSO<sub>4</sub>). Plates were incubated  
117 overnight at 40°C and plaques were counted (titration) or recorded (detection).

### 118 **Durability of resistance**

119 How can we measure the durability of a resistance? The durability of a resistance is  
120 defined as the time between its introduction at a large scale and its large circumvention  
121 by parasite when conditions are favorable for the parasite development [7]. Consequently,  
122 in absence a pre-existing escape parasite, the durability of a resistance depends on two  
123 factors: 1) the rate at which escape mutants are generated and 2) their spread into the  
124 host population. In the case of an homogeneous resistant host population, any viable  
125 escape mutants will inevitably spread quickly into the population. Therefore, in this  
126 simple case, the durability of a resistance depends mainly on the rate at which viable  
127 escape mutants appears. When escape mutants can only appear by mutation, measuring  
128 their rate of apparition is the same as measuring the mutation rate of parasite targeted  
129 sequence, here the PAM and seed sequences.

130

131 The viable mutation rate of a sequence can be measured using a Luria-Delbrück  
132 protocol. The durability of resistance of each of the 17 distincts BIM was measured  
133 using a three-steps Luria-Delbrück protocol (see supplemental informations C for a

134 graphic overview of the protocol). These measurements were replicated 3 times with 3  
135 independent clonal lysates of phage 2972. To ensure that pre-existing escape mutants  
136 have not altered these measurements, we measured for each BIM, the initial frequency of  
137 escape mutants. The frequency of pre-existing mutants to each of the 17 different BIMs  
138 was found to be below  $2.9 \times 10^{-5}$ . Because we inoculated a small quantity of phage 2972  
139 (see below), the impact of the standing genetic variance on the adaptation of the phage  
140 was assumed to be negligible.

141

142 In the first step of this protocol, for each BIM, WT phages were amplified in 96 inde-  
143 pendent replicates on the WT-phage-sensitive bacteria (i.e. in the absence of selection).  
144 In each replicate, 20  $\mu\text{L}$  of LM17+CaCl<sub>2</sub> were inoculated with 0.2  $\mu\text{L}$  of WT bacteria  
145 in mid-exponential phase, phages at a concentration of 300 PFU/20 $\mu\text{L}$  and incubated  
146 at 40°C for 24 hours. We confirmed by titrating four replicates before incubation that  
147  $N_i \approx 300$  PFU/20  $\mu\text{L}$  and we measured  $N_f$  by titrating 10 randomly chosen lysates. We  
148 found  $N_f \approx 1.72 \times 10^6$  PFU/20  $\mu\text{L}$ .

149

150 In the second step of the protocol, the bacteria from each replicate were pelleted down  
151 with a 5-minute centrifugation (6189g) (see supplementary information D) and 25%  
152 (5 $\mu\text{L}$ ) of the supernatant was inoculated into a 200  $\mu\text{L}$  culture of the focal BIM and  
153 incubated for 24 hours at 40°C. This second step ensured that even in replicates where  
154 the frequency of escape mutants was small at the end of the first step, the frequency of  
155 escape mutants would be sufficiently high to be detectable in the third step of the protocol.

156

157 In the final and third step of the protocol, the presence of escape phages in each  
158 individual replicate was assessed using phage detection assays.  $P_E$ , the probability of  
159 escape, was calculated as the fraction of replicates where phage escape was detectable. It  
160 is possible [28] to estimate the rate of escape mutations against each BIM using:

$$\mu = \frac{-\ln(1 - P_E)}{z(N_f - N_i)}$$

161 with  $\mu$  the mutation rate per target sequence (seed and PAM sequences),  $z$  the fraction  
162 of lysate used for the second amplification (here 1/4),  $N_f$  the final number of phages per  
163 replicate and  $N_i$  the initial number of phages per replicate. To further strengthen the  
164 results, the entire protocol has been triplicated with 3 independent clonal phage lysate.  
165 Therefore, for each BIM, the estimation of  $\mu$  comes from 288 independent lysates.

## 166 Relative fitness of phage escape mutants

167 For each of the 17 different BIMs, we selected at random 5 phage isolates that escaped  
168 bacterial resistance. A single plaque from each of these 5 isolates was amplified in liquid  
169 and re-isolated twice on plates, on the BIM on which they were isolated from. After  
170 amplification, phages and remaining bacteria were separated by filtration (0.2  $\mu\text{m}$ ) and  
171 phages were stored in 20% glycerol at  $-80^\circ\text{C}$ . Genome sequencing (see supplementary  
172 information E for the list of primers and F for their protospacer sequence) confirmed  
173 that all escape phages contained mutations in their PAM or their seed sequence. This  
174 protocol generated a collection of escape mutants for all BIMs.

175

176 The relative fitness of all the escape mutants was determined using triplicate competition  
177 experiments against a reference phage which contains a 37-bp deletion in its *orf24*  
178 (see supplemental information G). This deletion allowed us to readily distinguish the  
179 reference strain from all the other escape mutants (see section G in the supplementary  
180 information). Approximately 3 000 phages (50% escape mutant and 50% reference phage)  
181 were inoculated in 10 mL LM17+CaCl<sub>2</sub> supplemented with 100  $\mu\text{L}$  of WT bacteria in  
182 early stationary phase. After a 24 hour incubation at  $40^\circ\text{C}$ , the remaining bacteria were  
183 removed by filtration and phages were stored at  $-80^\circ\text{C}$ . Before and after amplification, the  
184 proportion of the tested phage was measured by qPCR (see section G in the supplementary  
185 information). The relative fitness of the escape mutant  $m$  was determined using:

$$s_m = r_m - r_{WT} = \log \left( \frac{p_f (1 - p_i)}{p_i (1 - p_f)} \right) - \log \left( \frac{p'_f (1 - p'_i)}{p'_i (1 - p'_f)} \right)$$

186 where  $r_m$  and  $r_{WT}$  refer to the malthusian growth rates of the escape mutant and the  
187 WT phage, respectively,  $p_i$  and  $p_f$  (respectively,  $p'_i$  and  $p'_f$ ) are the frequencies of the  
188 mutant phage before and after the competition (the prime refers to the frequency of the  
189 WT phage 2972).

## 190 Statistical analyses

191 All statistical analyses were run using R Software (version 3.3.2, [29]), through RStudio  
192 (Version 1.0.136). For mixed model, R package lme4 version 1.1-13 was used [30].

193

194 We performed an Analysis of Variance (ANOVA) to determine if the position of the  
195 protospacer on the phage genome impacts the durability of resistances.

196 [Linear](#) models were used for the analysis of relative fitness data. In the first model, we  
197 tested the effect of phage genotype on relative fitness. In the second model, we tested the

198 impact of mutation type (synonymous vs non-synonymous) on relative fitness of phages  
199 escaping the BIMs that target an *orf* (36 phage escape mutants). In the third model, we  
200 assessed the effect of the relative fitness of phage escape mutants on the durability of  
201 resistance of their respective BIM.

## 202 Results

203 To study the durability of various CRISPR alleles, we generated 17 different resistant  
204 strains (BIMs) characterized by a new and unique spacer within the CRISPR1 array.  
205 Each spacer targets a different protospacer, ie. a different part of the phage genome  
206 (supplemental data B). In total, 13 of the 44 phage genes (as well as some non-coding  
207 regions) were targeted by at least one spacer, leading to a good coverage of the phage  
208 genome by these 17 BIMs (Figure 1).

209  
210 Our measures of BIMs' durability using fluctuation tests, revealed considerable vari-  
211 ation in the ability of the phage to escape different BIMs (Figure 1, supplementary  
212 information H, ANOVA,  $F\text{-value} = 10.89$ ,  $df = 16$ ,  $p\text{-value} < 0.001$ ). We also used the  
213 probability of escape to estimate the mutation rates for each target sequence (seed and  
214 PAM sequences) (see supplementary information I). The average mutation rate was  
215 estimated to be  $3.4 \times 10^{-7}$  mutation/target sequence/replication and the escape rate of  
216 the less durable BIM was 123 times higher than the one of the most durable BIM.

217  
218 One possible explanation for the observed variation in durability of resistances is that  
219 there are differences in the fitness costs associated with these different escape mutations.  
220 Indeed, the Luria-Delbrück protocol used to measure the durability of resistances assume  
221 that phage escape mutations are neutral [31]. This assumption is unlikely to be met  
222 here and an heterogeneity in the fitness of the escape phage could explain the observed  
223 heterogeneity in durability. To explore this hypothesis, we isolated 40 phage mutants  
224 escaping the 17 distinct single CRISPR-resistances. A total of 35 escape phages carry  
225 a single bp mutation in the targeted sequence, 4 of the remaining phages carry double  
226 bp mutations in the targeted sequence, one escape phage has a single bp deletion (see  
227 supplementary information F). Among the substitutions, 27 are transversions, 12 are  
228 purine transitions and 4 pyrimidine transitions. Ten escape mutants were characterized  
229 by synonymous mutations (see supplementary information J).

230  
231 To measure fitness, we competed each of the escape phage mutants against a reference

232 phage and measure their relative abundance before and after the experiment. From these  
233 data, we deduce relative fitness. We found that relative fitness was highly variable, ranging  
234 from -6.21 to 0.68 with an average of -2.22 and a standard deviation of 1.71 (Figure 2,  
235 see supplementary information K). Although the majority of the phage escape mutants  
236 had a lower fitness than the WT phage (32/40), some escape mutants were neutral (8/40)  
237 (Figure 2, supplementary information K). The presence of non-synonymous mutations  
238 was not a good predictor of escape mutant fitness (t-value = -0.509, P(R>t) = 0.612)  
239 and all tested synonymous mutations but one lower phage fitness (see supplementary  
240 information L). Interestingly, we also found that escape mutant fitness was not a good  
241 predictor of the durability of each BIM (Figure 3, t-value = -0.423, P(R>t) = 0.673).  
242 Hence, the heterogeneity in the durability of CRISPR resistances is not caused by the  
243 heterogeneity of fitness costs associated with these escape mutations (see Figure 3).

## 244 Discussion

245 We studied the variation in the ability of the virulent phage 2972 to escape distinct resis-  
246 tance alleles at the CRISPR-Cas immune system of its host *S. thermophilus* DGCC7710.  
247 We found i) considerable variation in the durability among these different resistant strains  
248 (and therefore in the apparent mutation rate of phage protospacers) and ii) substantial  
249 variation in fitness among phages carrying escape mutations. Yet, the cost of those escape  
250 mutations was not associated with the durability of their respective resistance strains.  
251 If the fitness cost of escape mutations is not a good predictor of resistance durability  
252 what drives the variation in durability? We believe that two non-mutually exclusive  
253 processes could explain the observed patterns: (i) variation in the mutation rate along  
254 the phage genome and (ii) variation in the probability of generating lethal mutations  
255 among different sequences targeted by the CRISPR-Cas system.

256  
257 First, a variation in the mutation rate along the phage genome can result from an het-  
258 erogeneity of the replication machinery. Such a variation in mutation rates has previously  
259 been described in yeast [32], RNA viruses [33] and bacteria [34] but to our knowledge  
260 not yet in bacteriophages. The precise mechanism used by phage 2972 to replicate and  
261 repair its genome is unknown, limiting our ability to test this hypothesis. However, since  
262 phage 2972 encodes and expresses its own replication machinery and does not possess  
263 any repair mechanism [26, 35], it is tempting to hypothesize that no repair mechanisms  
264 are involved and that the entire replication is made by its replication machinery. This  
265 machinery could yield substantial variation among different parts of the phage genome.



266 Note, however, that most escape mutants we isolated were due to transversions instead  
267 of transitions (see supplementary information J), whereas most replication machineries  
268 show a biased pattern to transition [32, 36]. If a heterogeneous fidelity rate was at the  
269 origin of the observed heterogeneity in durability of resistances, 2972 machinery would  
270 have an unconventional mutation bias.

271

272 Second, variation in the frequency of lethal mutations along the phage genome could  
273 also contribute to the observed variation in BIM durability. Lethal mutations are very  
274 common and can reach up to 40% of viruses total mutations [37, 38, 39], but, to our  
275 knowledge, the heterogeneity of the probability of lethal mutation along the genome  
276 has not been studied. Because some genes are known to be essential while others are  
277 accessory (e.g. *orf39* and *orf41* are not expressed during an infection by phage 2972 [35]),  
278 we can expect that mutations in different genes should result in different fractions of  
279 lethal mutations and, consequently, in variations in the durability among BIMs targeting  
280 these different genes.

281

282 Additional experiments are required to evaluate the relative importance of the varia-  
283 tions in (i) mutation rate and (ii) the proportion of lethals along the phage genome on  
284 the durability of CRISPR resistance. The heterogeneity in the mutation rate could be  
285 assessed by measuring the durability of several spacers that target different non-functional  
286 coding regions of the phage genome. Phage 2972 carry such a sequence in the form  
287 of an incomplete lysogeny module that is not expressed [26, 35]. If we could create  
288 different BIMs targeting this module, any heterogeneity in durability among those BIMs  
289 would only result from an heterogeneity in the mutation rates among the different target  
290 sequences. To evaluate the alternative hypothesis that the variation in durability results  
291 from variation in the fraction of lethal mutants, one could measure directly this fraction  
292 of lethal mutants through the systematic introduction of point mutations in the target  
293 sequence of BIMs with contrasted levels of durability [37, 38, 39]. Thanks to recent  
294 progress in molecular biology, a range of mutants can be produced by systematically  
295 changing each of the nucleotide of the target sequence [40, 41]. The comparison of the  
296 number of lethal mutations for a durable and non-durable resistance would allow one to  
297 evaluate directly the impact of this factor on the variation of the durability.

298

299 CRISPR–Cas immunity is known to generate and maintain a high diversity of resistance  
300 alleles against the same phage [22, 42] and this diversity in resistance is known to limit  
301 the growth of the phage population [28, 42]. Theoretical models and experimental tests

302 indicate that such diversity limits the evolutionary emergence of the pathogens [28]. Yet,  
303 those studies ignore the heterogeneity in the durability of resistance among different  
304 alleles. Our results indicate that another potential benefit of generating this diversity is  
305 to explore a range of durability of resistance. The most durable alleles will outcompete  
306 the other BIMs and this may provide a very robust way to hamper the evolution of the  
307 phage. In addition to this inter-host diversity, a single cell can acquire more than one  
308 spacer against the same parasite. The acquisition of multiple spacers targeting different  
309 parts of the phage genome implies that the phage needs multiple mutations before it  
310 can infect this multiply resistant bacteria [43]. As most escape mutations are costly  
311 (Figure 2), carrying multiple escape mutations is likely to reduce dramatically the fitness  
312 of the phage. In contrast, the acquisition of multiple spacers does not alter the fitness  
313 of the bacteria [44]. This asymmetry may help explaining the ultimate extinction of  
314 phage populations coevolving with CRISPR–Cas immunity [22, 45]. It is also impor-  
315 tant to note that some phages have evolved the ability to defeat CRISPR immunity  
316 using anti-CRISPR proteins that inhibit the defense conferred by CRISPR–Cas [46, 47]  
317 (note that to our knowledge, phage 2972 does not carry any anti-CRISPR against *S.*  
318 *thermophilus* CRISPR systems). Even though anti-CRISPR can be partially efficient  
319 against CRISPR–Cas, the cooperation between phages ensures that, above a minimal  
320 concentration, phages can invade a resistant host population without acquiring escape  
321 mutations in the sequences targeted by CRISPR–Cas [48, 49].

322

323 *S. thermophilus* is widely used by the dairy industry for the manufacture of several  
324 fermented milk products (yoghurt, cheese) and the identification of BIMs with particularly  
325 durable resistance could have very practical implications. The use and/or the combination  
326 of these BIMs is likely to protect the starter cultures against phage infection. In addition,  
327 it would be particularly useful to identify durable spacers that target related phages.  
328 Such generalist spacers have been observed before [23]. The use of a durable generalist  
329 spacer could massively improve the resistance of *S. thermophilus* strains. Our biological  
330 model provides also a unique opportunity to evaluate experimentally the effectiveness of  
331 different intervention strategies on the long-term efficacy of resistance to pathogens. It  
332 may thus provide important insights for the implementation of sustainable management  
333 of pathogens and pests [4, 9, 28].

334

335 In addition to these applications in the dairy industry and in agriculture, the CRISPR-  
336 Cas9 technology can be used as a driving endonuclease, ie. a genetic tool that make  
337 an engineered allele spread into natural populations by non-mendelian heredity [50].

338 Indeed, in a heterozygote carrying a CRISPR-Cas9 and its guide, the endonuclease will  
339 target and cleave the homologous allele. As repair mechanism usually involve homologous  
340 DNA sequences, they will usually add a copy of the CRISPR-Cas9 and its guide at the  
341 place of the former allele, leading to the rapid spread of the CRISPR-Cas9/guide in  
342 the population[50, 51]. However, if the presence of CRISPR-Cas9 is costly for its host,  
343 it is likely that escape mutation will emerge and break the spread of the gene-drive  
344 [51, 52]. Our results indicate that the durability of gene-drive strategies targeting distinct  
345 genome regions is likely to be very variable. Understanding the ultimate source of the  
346 variation of durability is particularly important for the effectiveness of gene-drive based  
347 on CRISPR-Cas9.

348

## 349 **Acknowledgements**

350 The authors thank Alison Feder, Peter Grant, Olivier Tenaillon, Stéphanie Bedhomme,  
351 Oliver Kaltz, Elze Hesse, Matthias Grenié and H el ene Pidon for helpful discussions. The  
352 authors thank the qPHD, qPCR (head: Philippe Clair) and the GenSeq (head: Fr ed erique  
353 Cerqueira and Erick Desmarais) platforms of the University of Montpellier for their  
354 help. E.R.W. further acknowledges the Natural Environment Research Council (<https://nerc.ukri.org>) (NE/M018350/1), the BBSRC (BB/N017412/1), and the European  
355 Research Council (<https://erc.europa.eu>) (ERC-STG-2016-714478 - EVOIMMECH)  
356 for funding. SM acknowledges funding from the Natural Sciences and Engineering  
357 Research Council of Canada (Discovery Program). SM holds the Tier 1 Canada Research  
358 Chair in Bacteriophages. HC acknowledges funding from the EMBO (EMBO Short  
359 Term Fellowship 7191). SG acknowledges funding from the Leverhulme Trust (Visiting  
360 Professorships) and the CNRS (PEPS MPI grant).

## 362 **References**

- 363 [1] O'Neill (chair) J. Tackling drug-resistant infections globally: final report and recommendations. The  
364 review on antimicrobial resistance. Commissioned by the UK Prime Minister. 2016;Available from:  
365 <http://amr-review.org/Publications>.
- 366 [2] Feder AF, Rhee SY, Holmes SP, Shafer RW, Petrov DA, Pennings PS. More effective drugs lead  
367 to harder selective sweeps in the evolution of drug resistance in HIV-1. *eLife*. 2016 feb;5:e10670.  
368 Available from: <https://doi.org/10.7554/eLife.10670>.
- 369 [3] Ghany MG, Doo EC. Antiviral resistance and hepatitis B therapy. *Hepatology*. 2009;49(S5):S174-  
370 S184. Available from: <http://dx.doi.org/10.1002/hep.22900>.

- 371 [4] Leach JE, Cruz CMV, Bai J, Leung H. Pathogen fitness penalty as a predictor of durability of  
372 disease resistance genes. Annual Review of Phytopathology. 2001;39(1):187–224. Available from:  
373 <https://doi.org/10.1146/annurev.phyto.39.1.187>.
- 374 [5] Gandon S, Michalakis Y. Evolution of parasite virulence against qualitative or quantitative host  
375 resistance. Proceedings of the Royal Society of London B: Biological Sciences. 2000;267(1447):985–990.  
376 Available from: <http://rsob.royalsocietypublishing.org/content/267/1447/985>.
- 377 [6] Gandon S, Mackinnon MJ, Nee S, Read AF. Imperfect vaccines and the evolution of pathogen  
378 virulence. Nature. 2001 12;414:751. Available from: <https://www.nature.com/articles/414751a>.
- 379 [7] Johnson R. A critical analysis of durable resistance. Annual Review of Phytopathology. 1984;22(1):309–  
380 330. Available from: <https://doi.org/10.1146/annurev.py.22.090184.001521>.
- 381 [8] Kennedy DA, Read AF. Why does drug resistance readily evolve but vaccine resistance does not?  
382 Proceedings of the Royal Society of London B: Biological Sciences. 2017;284(1851). Available from:  
383 <http://rsob.royalsocietypublishing.org/content/284/1851/20162562>.
- 384 [9] Mundt CC. Durable resistance: A key to sustainable management of pathogens and pests. Infection,  
385 Genetics and Evolution. 2014;27:446 – 455. Available from: [http://www.sciencedirect.com/  
386 science/article/pii/S1567134814000148](http://www.sciencedirect.com/science/article/pii/S1567134814000148).
- 387 [10] Johnson R. Durable resistances: definition of, genetic control, and attainment in plant breeding.  
388 Phytopathology. 1981;71(6):567–568. Available from: [https://www.apsnet.org/publications/  
389 phytopathology/backissues/Documents/1981Articles/Phyto71n06\\_567.PDF](https://www.apsnet.org/publications/phytopathology/backissues/Documents/1981Articles/Phyto71n06_567.PDF).
- 390 [11] McDonald BA, Linde C. Pathogen population genetics, evolutionary potential, and durable resistance.  
391 Annual Review of Phytopathology. 2002;40(1):349–379. Available from: [https://doi.org/10.1146/  
392 annurev.phyto.40.120501.101443](https://doi.org/10.1146/annurev.phyto.40.120501.101443).
- 393 [12] Flor HH. Current status of the gene-for-gene concept. Annual Review of Phytopathology.  
394 1971;9(1):275–296. Available from: <https://doi.org/10.1146/annurev.py.09.090171.001423>.
- 395 [13] Stuthman DD, Leonard KJ, Miller-Garvin J. Breeding crops for durable resistance to disease.  
396 vol. 95 of Advances in Agronomy. Academic Press; 2007. p. 319 – 367. Available from: [http://  
397 www.sciencedirect.com/science/article/pii/S006521130795004X](http://www.sciencedirect.com/science/article/pii/S006521130795004X).
- 398 [14] Poland JA, Balint-Kurti PJ, Wisser RJ, Pratt RC, Nelson RJ. Shades of gray: the world of  
399 quantitative disease resistance. Trends in Plant Science. 2009 2018/09/02;14(1):21–29. Available  
400 from: <https://www.sciencedirect.com/science/article/pii/S1360138508002975>.
- 401 [15] Lafforgue G, Martínez F, Niu QW, Chua NH, Daròs JA, Elena SF. Improving the effectiveness of  
402 artificial microRNA (amiR)-mediated resistance against Turnip Mosaic Virus by combining two amiRs  
403 or by targeting highly conserved viral genomic regions. Journal of Virology. 2013;87(14):8254–8256.  
404 Available from: <http://jvi.asm.org/content/87/14/8254.abstract>.
- 405 [16] Kousik CS, Ritchie DF. Development of bacterial spot on near-isogenic lines of bell pepper  
406 carrying gene pyramids composed of defeated major resistance genes. Phytopathology. 1999  
407 2018/07/03;89(11):1066–1072. Available from: [https://doi.org/10.1094/PHYTO.1999.89.11.  
408 1066](https://doi.org/10.1094/PHYTO.1999.89.11.1066).
- 409 [17] Brun H, Levivier S, Somda I, Ruer D, Renard M, Chèvre AM. A field method for evaluating  
410 the potential durability of new resistance sources: application to the *Leptosphaeria maculans*-  
411 *Brassica napus* pathosystem. Phytopathology. 2000 2018/07/03;90(9):961–966. Available from:  
412 <https://doi.org/10.1094/PHYTO.2000.90.9.961>.

- 413 [18] Labrie SJ, Samson JE, Moineau S. Bacteriophage resistance mechanisms. *Nat Rev Micro*. 2010  
414 03;8(5):317–327. Available from: <https://www.nature.com/articles/nrmicro2315>.
- 415 [19] Goldfarb T, Sberro H, Weinstock E, Cohen O, Doron S, Charpak-Amikam Y, et al. BREX is a novel  
416 phage resistance system widespread in microbial genomes. *The EMBO Journal*. 2015;34(2):169–183.  
417 Available from: <http://emboj.embopress.org/content/34/2/169>.
- 418 [20] Ofir G, Melamed S, Sberro H, Mukamel Z, Silverman S, Yaakov G, et al. DISARM is a widespread  
419 bacterial defence system with broad anti-phage activities. *Nature Microbiology*. 2018;3(1):90–98.  
420 Available from: <https://www.nature.com/articles/s41564-017-0051-0>.
- 421 [21] Doron S, Melamed S, Ofir G, Leavitt A, Lopatina A, Keren M, et al. Systematic discovery of  
422 antiphage defense systems in the microbial pangenome. *Science*. 2018;359(6379). Available from:  
423 <http://science.sciencemag.org/content/359/6379/eaar4120>.
- 424 [22] Paez-Espino D, Morovic W, Sun CL, Thomas BC, Ueda Ki, Stahl B, et al. Strong bias in the  
425 bacterial CRISPR elements that confer immunity to phage. *Nature Communications*. 2013;4:1430.  
426 Available from: <https://www.nature.com/articles/ncomms2440>.
- 427 [23] Barrangou R, Fremaux C, Deveau H, Richards M, Boyaval P, Moineau S, et al. CRISPR provides  
428 acquired resistance against viruses in prokaryotes. *Science*. 2007;315(5819):1709. Available from:  
429 <http://science.sciencemag.org/content/315/5819/1709>.
- 430 [24] Horvath P, Romero DA, Coûté-Monvoisin AC, Richards M, Deveau H, Moineau S, et al. Diversity,  
431 activity, and evolution of CRISPR loci in *Streptococcus thermophilus*. *Journal of Bacteriology*.  
432 2008 02;190(4):1401–1412. Available from: <https://onlinelibrary.wiley.com/doi/abs/10.1111/j.1462-2920.2012.02879.x>.
- 434 [25] Sun CL, Barrangou R, Thomas BC, Horvath P, Fremaux C, Banfield JF. Phage mutations in response  
435 to CRISPR diversification in a bacterial population. *Environmental Microbiology*. 2013;15(2):463–470.  
436 Available from: <https://onlinelibrary.wiley.com/doi/abs/10.1111/j.1462-2920.2012.02879.x>.
- 438 [26] Lévesque C, Duplessis M, Labonté J, Labrie S, Fremaux C, Tremblay D, et al. Genomic organization  
439 and molecular analysis of virulent bacteriophage 2972 infecting an exopolysaccharide-producing  
440 *Streptococcus thermophilus* strain. *Applied and Environmental Microbiology*. 2005 07;71(7):4057–4068.  
441 Available from: <https://aem.asm.org/content/71/7/4057>.
- 442 [27] Hynes AP, Lemay ML, Trudel L, Deveau H, Frenette M, Tremblay DM, et al. Detecting natural  
443 adaptation of the *Streptococcus thermophilus* CRISPR-Cas systems in research and classroom settings.  
444 *Nature Protocols*. 2017 02;12:547. Available from: <http://dx.doi.org/10.1038/nprot.2016.186>.
- 445 [28] Chabas H, Lion S, Nicot A, Meaden S, van Houte S, Moineau S, et al. Evolutionary emergence of  
446 infectious diseases in heterogeneous host populations. *PLOS Biology*. 2018 09;16(9):1–20. Available  
447 from: <https://doi.org/10.1371/journal.pbio.2006738>.
- 448 [29] R Core Team. R: A language and environment for statistical computing. Vienna, Austria; 2016.  
449 Available from: <https://www.R-project.org/>.
- 450 [30] Bates D, Mächler M, Bolker B, Walker S. Fitting linear mixed-effects models using lme4. *Journal of*  
451 *Statistical Software*. 2015;67(1):1–48. Available from: <https://www.jstatsoft.org/article/view/v067i01>.
- 453 [31] Luria SE, Delbrück M. Mutations of bacteria from virus sensitivity to virus resistance. *Genetics*.  
454 1943;28(6):491–511. Available from: <http://www.genetics.org/content/28/6/491>.

- 455 [32] Lujan SA, Clausen AR, Clark AB, MacAlpine HK, MacAlpine DM, Malc EP, et al. Heteroge-  
456 neous polymerase fidelity and mismatch repair bias genome variation and composition. *Genome*  
457 *Research*. 2014;24(11):1751–1764. Available from: <http://genome.cshlp.org/content/24/11/1751>.  
458 **abstract**.
- 459 [33] Geller R, Estada Ú, Peris JB, Andreu I, Bou JV, Garijo R, et al. Highly heterogeneous mutation  
460 rates in the hepatitis C virus genome. *Nature Microbiology*. 2016 04;1:16045 EP –. Available from:  
461 <http://dx.doi.org/10.1038/nmicrobiol.2016.45>.
- 462 [34] Dillon MM, Sung W, Lynch M, Cooper VS. Periodic Variation of Mutation Rates in Bacterial  
463 Genomes Associated with Replication Timing. *mBio*. 2018;9(4). Available from: [https://mbio.asm](https://mbio.asm.org/content/9/4/e01371-18).  
464 [org/content/9/4/e01371-18](https://mbio.asm.org/content/9/4/e01371-18).
- 465 [35] Young JC, Dill BD, Pan C, Hettich RL, Banfield JF, Shah M, et al. Phage-induced expression of  
466 CRISPR-associated proteins is revealed by shotgun proteomics in *Streptococcus thermophilus*. *PLOS*  
467 *ONE*. 2012 05;7(5):1–12. Available from: <https://doi.org/10.1371/journal.pone.0038077>.
- 468 [36] Hestand MS, Houdt JV, Cristofoli F, Vermeesch JR. Polymerase specific error rates and profiles  
469 identified by single molecule sequencing. *Mutation Research/Fundamental and Molecular Mechanisms*  
470 *of Mutagenesis*. 2016;784-785:39 – 45. Available from: [http://www.sciencedirect.com/science/](http://www.sciencedirect.com/science/article/pii/S0027510716300045)  
471 [article/pii/S0027510716300045](http://www.sciencedirect.com/science/article/pii/S0027510716300045).
- 472 [37] Sanjuán R, Moya A, Elena SF. The distribution of fitness effects caused by single-nucleotide  
473 substitutions in an RNA virus. *Proceedings of the National Academy of Sciences*. 2004;101(22):8396–  
474 8401. Available from: <http://www.pnas.org/content/101/22/8396>.
- 475 [38] Domingo-Calap P, Cuevas JM, Sanjuán R. The fitness effects of random mutations in single-  
476 stranded DNA and RNA bacteriophages. *PLOS Genetics*. 2009;5(11):1–7. Available from: <https://doi.org/10.1371/journal.pgen.1000742>.  
477
- 478 [39] Peris JB, Davis P, Cuevas JM, Nebot MR, Sanjuán R. Distribution of fitness effects caused by  
479 single-nucleotide substitutions in bacteriophage  $\phi$ 1. *Genetics*. 2010;185(2):603–609. Available from:  
480 <http://www.genetics.org/content/185/2/603>.
- 481 [40] Martel B, Moineau S. CRISPR-Cas: an efficient tool for genome engineering of virulent bacteriophages.  
482 *Nucleic Acids Research*. 2014;42(14):9504–9513. Available from: [http://dx.doi.org/10.1093/nar/](http://dx.doi.org/10.1093/nar/gku628)  
483 [gku628](http://dx.doi.org/10.1093/nar/gku628).
- 484 [41] Lemay ML, Tremblay DM, Moineau S. Genome engineering of virulent lactococcal phages using  
485 CRISPR-Cas9. *ACS Synthetic Biology*. 2017;6(7):1351–1358. Available from: [https://doi.org/10.](https://doi.org/10.1021/acssynbio.6b00388)  
486 [1021/acssynbio.6b00388](https://doi.org/10.1021/acssynbio.6b00388).
- 487 [42] van Houte S, Ekroth AKE, Broniewski JM, Chabas H, Ashby B, Bondy-Denomy J, et al. The  
488 diversity-generating benefits of a prokaryotic adaptive immune system. *Nature*. 2016 04;532:385.  
489 Available from: <http://dx.doi.org/10.1038/nature17436>.
- 490 [43] Deveau H, Barrangou R, Garneau JE, Labonté J, Fremaux C, Boyaval P, et al. Phage response to  
491 CRISPR-encoded resistance in *Streptococcus thermophilus*. *Journal of Bacteriology*. 2008;190(4):1390–  
492 1400. Available from: <http://jbs.asm.org/content/190/4/1390.abstract>.
- 493 [44] Vale PF, Lafforgue G, Gatchitch F, Gardan R, Moineau S, Gandon S. Costs of CRISPR-Cas-mediated  
494 resistance in *Streptococcus thermophilus*. *Proceedings of the Royal Society of London B: Biological*  
495 *Sciences*. 2015;282(1812). Available from: [http://rspb.royalsocietypublishing.org/content/](http://rspb.royalsocietypublishing.org/content/282/1812/20151270)  
496 [282/1812/20151270](http://rspb.royalsocietypublishing.org/content/282/1812/20151270).

- 497 [45] Weissman JL, Holmes R, Barrangou R, Moineau S, Fagan WF, Levin B, et al. Immune loss as  
498 a driver of coexistence during host-phage coevolution. *The Isme Journal*. 2018 01;12:585 EP –.  
499 Available from: <http://dx.doi.org/10.1038/ismej.2017.194>.
- 500 [46] Bondy-Denomy J, Pawluk A, Maxwell KL, Davidson AR. Bacteriophage genes that inactivate  
501 the CRISPR/Cas bacterial immune system. *Nature*. 2012 12;493:429. Available from: <http://dx.doi.org/10.1038/nature11723>.  
502
- 503 [47] Hynes AP, Rousseau GM, Agudelo D, Goulet A, Amigues B, Loehr J, et al. Widespread anti-  
504 CRISPR proteins in virulent bacteriophages inhibit a range of Cas9 proteins. *Nature Communications*.  
505 2018;9(1):2919. Available from: <https://doi.org/10.1038/s41467-018-05092-w>.
- 506 [48] Landsberger M, Gandon S, Meaden S, Rollie C, Chevallereau A, Chabas H, et al. Anti-CRISPR  
507 phages cooperate to overcome CRISPR-Cas immunity. *Cell*. 2018 2018/08/30;174(4):908–916.e12.  
508 Available from: <https://doi.org/10.1016/j.cell.2018.05.058>.
- 509 [49] Borges AL, Zhang JY, Rollins MF, Osuna BA, Wiedenheft B, Bondy-Denomy J. Bacteriophage  
510 cooperation suppresses CRISPR-Cas3 and Cas9 immunity. *Cell*. 2018 2018/08/30;174(4):917–925.e10.  
511 Available from: <https://doi.org/10.1016/j.cell.2018.06.013>.
- 512 [50] Godfray HCJ, North A, Burt A. How driving endonuclease genes can be used to combat pests  
513 and disease vectors. *BMC Biology*. 2017 Sep;15(1):81. Available from: <https://doi.org/10.1186/s12915-017-0420-4>.  
514
- 515 [51] Noble C, Adlam B, Church GM, Esvelt KM, Nowak MA. Current CRISPR gene drive systems  
516 are likely to be highly invasive in wild populations. *eLife*. 2018 jun;7:e33423. Available from:  
517 <https://doi.org/10.7554/eLife.33423>.
- 518 [52] Unckless RL, Clark AG, Messer PW. Evolution of resistance against CRISPR/Cas9 gene drive.  
519 *Genetics*. 2017;205(2):827–841. Available from: <http://www.genetics.org/content/205/2/827>.

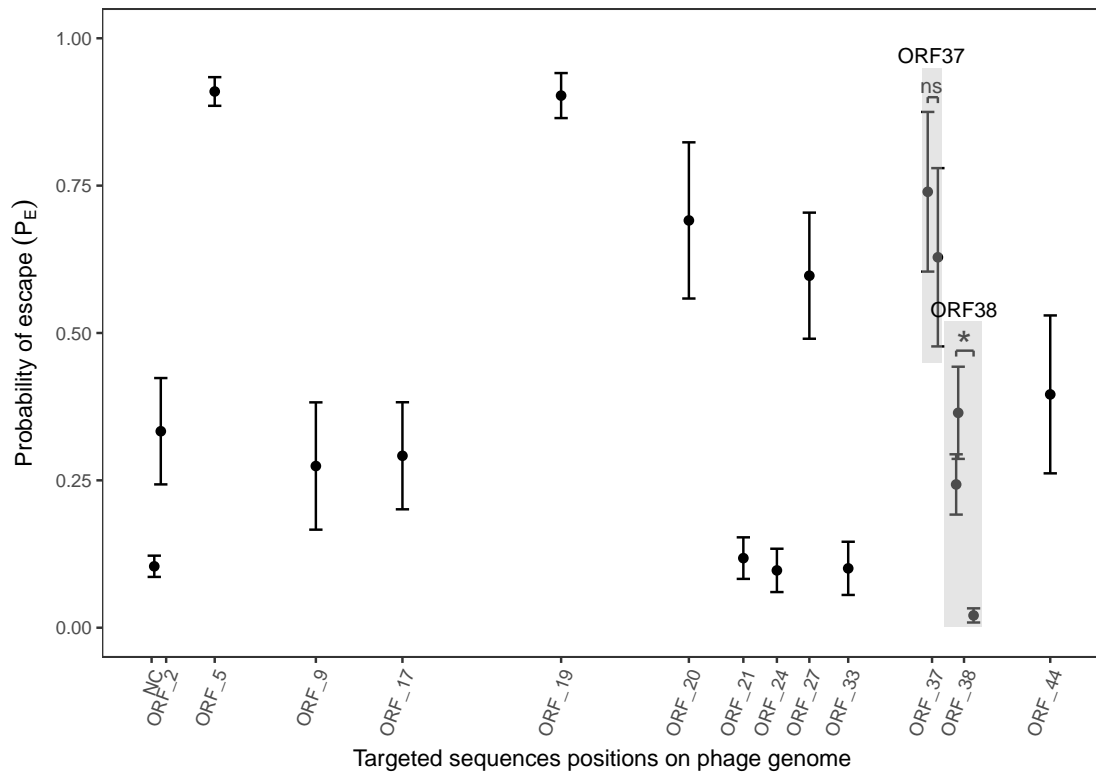


Figure 1: **Variability in the durability of CRISPR–Cas immunity.**

The mutation rate of 17 protospacers whose positions are labelled on the x-axis were measured using fluctuation tests.  $P_E$  values, ie. the number of replicates in which a phage escape mutant evolved, are reported and show heterogeneity among the targeted sequences, implying that there is heterogeneity in the durability of CRISPR–Cas resistances. The two protospacers of *orf37* have the same mutation rate but at least one of the protospacer of *orf38* has a lower mutation rate.



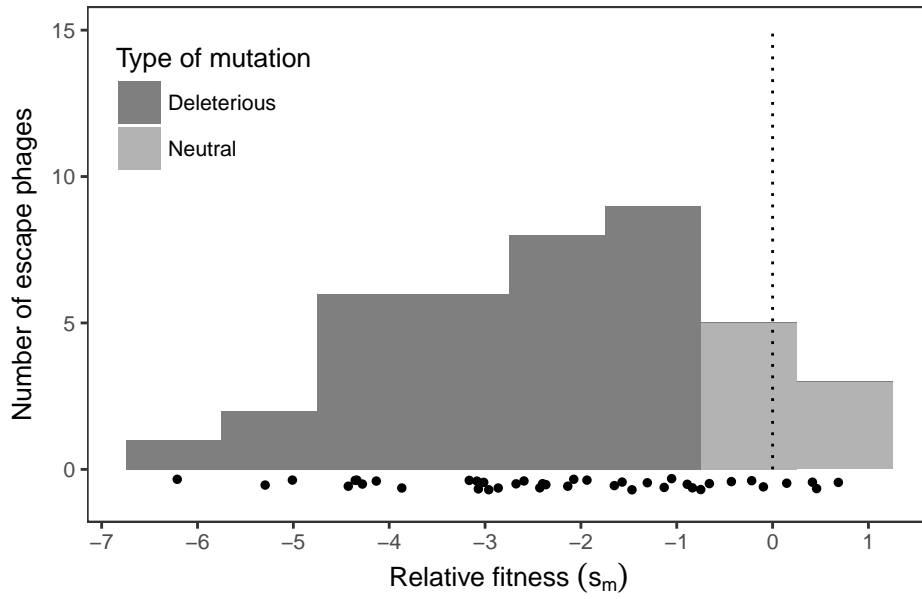


Figure 2: **Distribution of fitness effects of escape mutations in the phage.**

Relative fitness was measured through competition experiments with a collection of 40 escape phages, mutated on their seed or PAM sequences. Phages that carry a neutral and deleterious mutations are represented in medium and dark grey respectively. Black dots show the relative fitness of each escape phage. The dotted segment represents the fitness of WT phage 2972. Fitness value of each escape phage is also provided in the supplementary informations K.

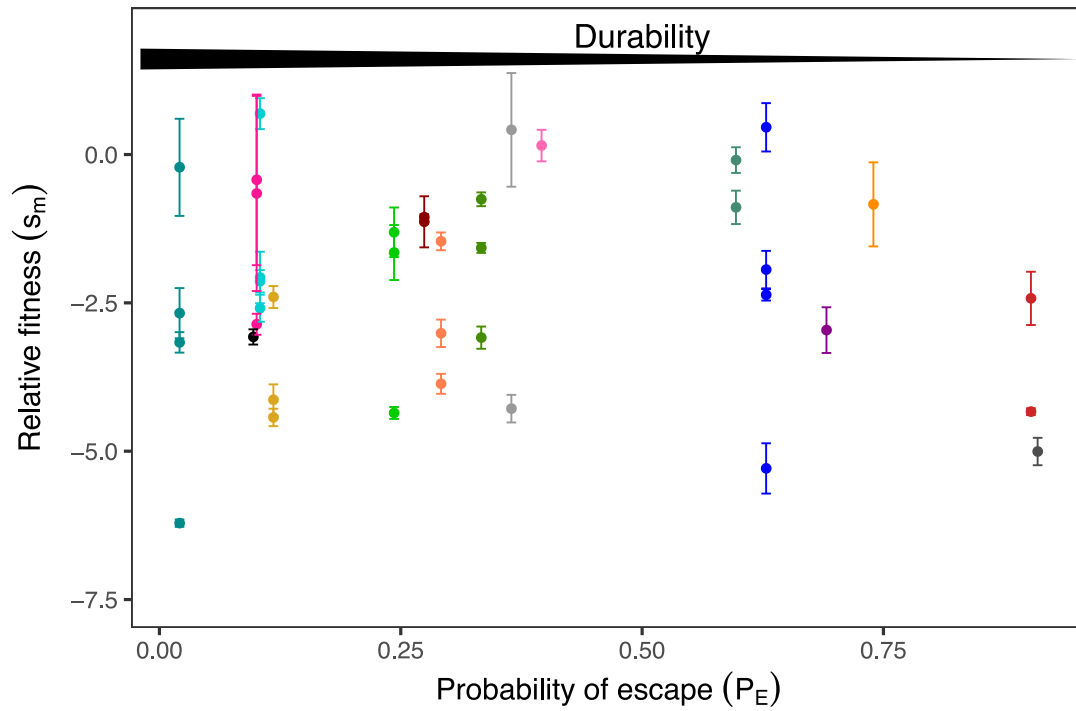


Figure 3: **Relative fitness of phage escape mutants against durability (probability of escape  $P_E$ ) of their respective BIM.**

Each color corresponds to a single BIM and each dot to a single escape phage. Error bars correspond to 95% Confidence Intervals. Raw data are provided in supplementary informations I and K.

# Supplementary informations

## 522 A. Primers used for CRISPR PCR and sequencing

### 523 A.1. PCR Protocol

524 The PCR mix contained 5  $\mu\text{L}$  of Multiplex Qiagen, 1  $\mu\text{L}$  of each primer, 2  $\mu\text{L}$  of sterile  
 525 water and 1  $\mu\text{L}$  of 1% bacteria. The PCR program involves 15 minutes at 94°C, 35 cycles  
 526 of 30 seconds at 94°C, 90 seconds at 60°C (CRISPR1 and 2) or 56°C (CRISPR3 and 4),  
 527 1 minute at 72°C and ended by 10 minutes at 60°C.

### 528 A.2. Primers

Table S1: Primer sequences used for the PCR of *S. thermophilus* loci.

CRISPR	Forward Primer (5'-3')	Reverse primer (5'-3')
1	TGCTGAGACAACCTAGTCTCTC	GGATCCGGATCCGTTGAGGCCTTG TTC
2	GCCCCTACCATAGTGCTGAAAAATTAG	CCAAATCTTGTGCAGGATGGTCG
3	GGTGACAGTCACATCTTGTCTAAAACG	GCTGGATATTCGTATAACATGTC
4	CCTCATAGAGCTTTGAAAGATGCTAGAC	GTTCTTCTTGATGCTTGTCGAGGC

## B. Characterization of BIMs

Table S2: BIMs spacer sequence and protospacer position in 2972 phage genome.

BIMs are named with the following nomenclature: NC or ORF indicates if the BIM targets a non-coding or a coding sequence respectively. When appropriate, the number following the \_ sign indicates the targeted *orf*. If multiple BIMs target the same *orf*, they are distinguished by capital letters.

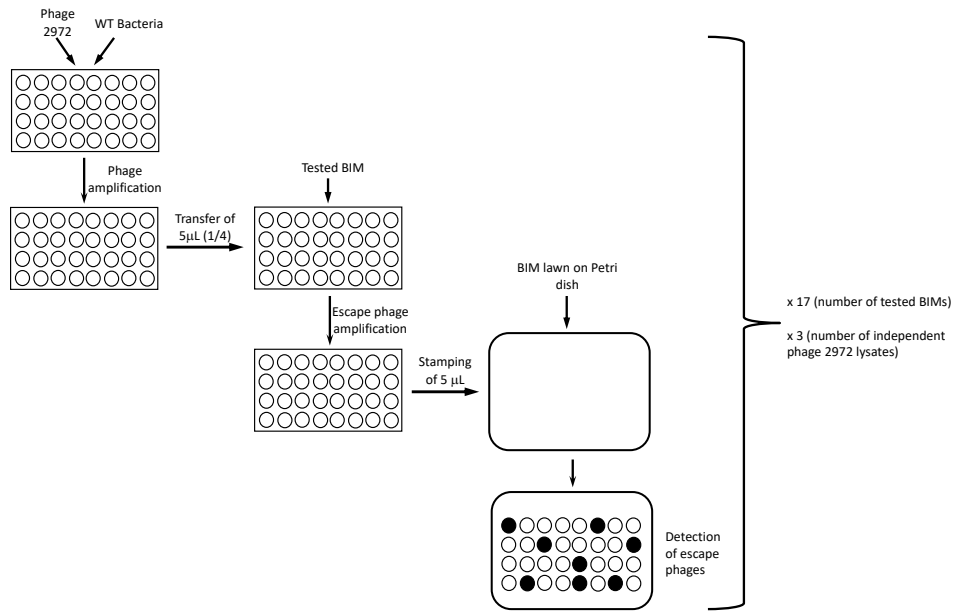
Name	Spacer sequence (5'-3')	Protospacer position in the phage genome	<i>orf</i> targeted in the phage genome
NC	AGGAGGTGGACATATTGGGCTAAATCAACG	954 – 983	non-coding
ORF_2	GCTCTACGACTTCTTCCACGAGTTCCTGCC	1 199 – 1 228	2
ORF_5	CCATCTCGTTGTCCTTACGACGACCAGACT	3 223 – 3 252	5
ORF_9	AGATATTGATTATGGTGTTAAAGCAGACCA	7 020 – 7 049	9
ORF_17	AAGCAAGTTGATATATTTCTCTTTCTTTAT	10 270 – 10 299	17
ORF_19	TTATCTGATTTTTTCCCCTTGATTCGGGG	16 226 – 16 255	19
ORF_20	TAAGGCAAACGAGACCGAGAGAGCTGCAGC	21 022 – 21 051	20
ORF_21	TTGACGATTGGGAACCGTGGAAGGAATTTG	23 067 – 23 096	21
ORF_24	AACACAGATGTTTTAGACCATGCGCAGAAG	24 326 – 24 355	24 + non-coding
ORF_27	TATTTGTACGTGAGTGGAAGTGCTTAGACT	25 544 – 25 473	27 + non-coding
ORF_33	TTTCATCGTCAATTTCCATGTTATAAATCT	27 003 – 27 032	33
ORF_37_A	TCGTTTTTCAGTCATTGGTGGTTTGTCAGCG	29 988 – 30 017	37

Continued on next page.

Name	Spacer sequence (5'-3')	Protospacer position in the phage genome	<i>orf</i> targeted in the phage genome
ORF_37_B	AGAAGCACCTCTTGCGTTGATAAAAGTATT	30 369 – 30 398	37
ORF_38_A	ATATTCATATTCCTGCTCATGTTTGATAG	31 055 – 31 084	38
ORF_38_B	CTTTATACTCGTTAAGAATGGCATCTACGA	31 132 – 31 161	38
ORF_38_C	CACATATCGACGTATCGTGATTATCCCATT	31 709 – 31 737	38
ORF_44	AGCCTAGATAGCGAAGTTGATCGTATCTAT	34 587 – 34 616	44

530

### C. Graphic overview of Luria-Delbrück protocol



533 **D. Impact of centrifugation on phage titre in lysate**

Table S3: Impact of centrifugation on phage titre. Centrifugation does not modify phage titre.

Titre before centrifugation (PFU/mL)	Titre after centrifugation (PFU/mL)
$8.2 \times 10^8$	$5.6 \times 10^8$
$1.0 \times 10^9$	$7.8 \times 10^8$
$1.2 \times 10^9$	$6.6 \times 10^8$
$9.2 \times 10^8$	$9.2 \times 10^8$

534 W=14.5, p-value=0.081 : No statistical differences in phage titer before and after  
535 centrifugation.

## E. Primers used for escape phages sequencing

Table S4: **Primers used for sequencing escape phages.**

Phages are named with the following nomenclature: 2972 indicates that it is a phage derived from 2972 phage; NC or ORF indicates whether the protospacer is part of a non-coding or a coding sequence respectively. When appropriate, the number following the \_ sign indicates the *orf* in which the protospacer is located. If a given *orf* contains several protospacers, they are distinguished by a capital letter.

Phage	Left Primer	Right Primer
2972_NC	TAGCGGAATTTTCACGGTCT	CCTGTAGCGGCATTTAGCTC
2972_ORF_2	CTTGCTTAGCCGTTGGGTAG	GGCTCATTTGTGGGTTGTCT
2972_ORF_5	CGGATAGGATTGCCAGCTAA	GTCATCGGTAGCACAGAGCA
2972_ORF_9	AAAACGACCGTCAACAGCTT	GTAGATGCAGCCTTGCGAAT
2972_ORF_17	AGAGCGCTAGACATGCCATT	AGAGGCGACCGAGTAAGTGA
2972_ORF_19	TCAGAGCCTTGCACAACATC	GCGGCACTTTCTTGTATGGT
2972_ORF_20	AGAGATGGAAGCCAAAGCAA	AAGATCCCGTTCTCGATGTG
2972_ORF_21	ATGGAAAGCCTAGCGTTGAA	TGTGGCTAGCTCCTTCGTTT
2972_ORF_24	TCGGATTGCTACCGAAAATC	CAATCTGCTCCACTGCGTTA
2972_ORF_27	AATACCGTGCCAAGTCTGGT	GGGATCCATTTTCTCATTACT
2972_ORF_33	AATGTCTGCCTCAAGCGACT	GTGTGCGGAGTGCAACTAAA
2972_ORF_37_A	CTTGCATGTTCCCAATTCCT	ACCGATATCCCACCTCCAGA
2972_ORF_37_B	AAGGAATTGGGAACATGCAA	ACTCGGCTAGGGCGTTATTT
2972_ORF_38_A	TCCCATCCGTTTATGGTAGG	ACCCTCGAAAATGGGAAAGT
2972_ORF_38_B	ACCCTCGAAAATGGGAAAGT	TCCCATCCGTTTATGGTAGG
2972_ORF_38_C	TTGCCATTATCGAAGGGAAG	CGAGTGGAACGACATCTGA
2972_ORF_44	TCGCAAGGAAATCCAAGAGT	CGTTTAACTTTCTTTTCAAGA



## F. Sequences of escape phages protospacer

Table S5: Sequences of escape phages protospacer and PAM. Mutations are highlighted in grey and their PAM is framed. WT and lower case letters indicate if the sequence corresponds to the WT phage 2972 or an escape mutant.

Phage escape mutants	Protospacer + PAM
2972_NC_WT	AGGAGGTGGACATATTGGGCTAAATCAACGACAGAA
2972_NC_a	AGGAGGTGGACATATTGGGCTAAATCGACGACAGAA
2972_NC_c	AGGAGGTGGACATATTGGGCTAAATCAACGACAGAG
2972_NC_d	AGGAGGTGGACATATTGGGCTAAAACAACGACAGAA
2972_NC_e	AGGAGGTGGACATATTGGGCTAAATCAACGACAGAA
2972_ORF_2_WT	GCTCTACGACTTCTTCCACGAGTTCCTGCCTCAGAA
2972_ORF_2_a	GCTCTACGACTTCTTCCACGAGTTCCTGCCTCATAA
2972_ORF_2_b	GCTCTACGACTTCTTCCACGAGTTCCTGCCTCAAAA
2972_ORF_2_c	GCTCTACGACTTCTTCCACGAGTTCCTTCCTCAGAA
2972_ORF_5_WT	CCATCTCGTTGTCCTTACGACGACCAGACTTGAGAA
2972_ORF_5_a	CCATCTCGTTGTCCTTACGACGACCAACTTGAGAA
2972_ORF_9_WT	AGATATTGATTATGGTGTAAAGCAGACCATAAGAA
2972_ORF_9_a	AGATATTGATTATGGTGTAAAGCAGAGCATAAGAA
2972_ORF_9_b	AGATATTGATTATGGTGTAAAGCAGAAAATAAGAA
2972_ORF_17_WT	AAGCAAGTTGATATATTTCTCTTTCTTTATTAAGAA
2972_ORF_17_a	AAGCAAGTTGATATATTTCTCTTTCTTTATTAAGAG
2972_ORF_17_b	AAGCAAGTTGATATATTTCTCTTTCTTTGTTAAGAA
2972_ORF_17_d	AAGCAAGTTGATATATTTCTCTTTCTTTATTAATAA
2972_ORF_19_WT	TTATCTGATTTTTTCCCCTTGATTTTCGGGGATAGAA
2972_ORF_19_a	TTATCTGATTTTTTCCCCTTGATTTTCGGGATAGAA
2972_ORF_19_b	TTATCTGATTTTTTCCCCTTGATTTCTTGGATAGAA
2972_ORF_20_WT	TAAGGCAAACGAGACCGAGAGAGCTGCAGCCGAGAA
2972_ORF_20_b	TAAGGCAAACGAGACCGAGAGAGCTGCAGCCGAGAC
2972_ORF_21_WT	TTGACGATTGGGAACCGTGGAAGGAATTTGCAAGAA
2972_ORF_21_a	TTGACGATTGGGAACCGTGGAAGGAATTTGCAAGAC
2972_ORF_21_c	TTGACGATTGGGAACCGTGGAAGGAATTTGCAAGTA
2972_ORF_21_d	TTGACGATTGGGAACCGTGGAAGGAATTTGCAAAAA

Continued on next page.

Phage escape mutants	Protospacer + PAM
2972_ORF_24_WT	AACACAGATGTTTTAGACCATGCGCAGAAGGG(AGAA)
2972_ORF_24_c	AACACAGATGTTTTAGACCATGCGCAGA-GGG(AGAA)
2972_ORF_27_WT	TATTTGTACGTGAGTGGAAGTGCTTAGACTTT(AGAA)
2972_ORF_27_a	TATTTGTACGTGAGTGGAAGTGCTTAGACTTT(AAAA)
2972_ORF_27_d	TATTTGTACGTGAGTGGAAGTGCTTAGTCTTT(AGAA)
2972_ORF_33_WT	TTTCATCGTCAATTTCCATGTTATAAATCTCT(AGAA)
2972_ORF_33_a	TTTCATCGTCAATTTCCATGTTATAAATCTCT(AAAA)
2972_ORF_33_b	TTTCATCGTCAATTTCCATGTTATAAATCTCT(TGAA)
2972_ORF_33_c	TTTCATCGTCAATTTCCATGTTATAAATTTCT(AAAA)
2972_ORF_37_A_WT	TCGTTTTTCAGTCATTGGTGGTTTGTTCAGCGAA(AGAA)
2972_ORF_37_A_a	TCGTTTTTCAGTCATTGGTGGTTTGTTCAGCGAA(AGAG)
2972_ORF_37_B_WT	AGAAGCACCTCTTGCGTTGATAAAAAGTATTGC(AGAA)
2972_ORF_37_B_a	AGAAGCACCTCTTGCGTTGATAAAAAGT(TTTGC)(AGAA)
2972_ORF_37_B_b	AGAAGCACCTCTTGCGTTGATAAAAAGCATTGC(AGAA)
2972_ORF_37_B_c	AGAAGCACCTCTTGCGTTGATAAAAAGTATTGC(AAAA)
2972_ORF_37_B_d	AGAAGCACCTCTTGCGTTGATAAAAATTTATTGC(AGAA)
2972_ORF_38_A_WT	ATATTCATATTCCCTGCTCATGTTTGATAGCA(AGAA)
2972_ORF_38_A_a	ATATTCATATTCCCTGCTCATGTTTGAAAGCA(AGAA)
2972_ORF_38_A_b	ATATTCATATTCCCTGCTCATGTTTGTTAGCA(AGAA)
2972_ORF_38_A_e	ATATTCATATTCCCTGCTCATGTTTGGATAGCA(AGAA)
2972_ORF_38_B_WT	CTTTATACTCGTTAAGAATGGCATCTACGACA(AGAA)
2972_ORF_38_B_a	CTTTATACTCGTTAAGAATGGCATCTTCGACA(AGAA)
2972_ORF_38_B_c	CTTTATACTCGTTAAGAATGGCATCTACGACA(ATAA)
2972_ORF_38_C_WT	ACATATCGACGTATCGTGATTATCCCATTCA(AGAA)
2972_ORF_38_C_a	ACATATCGACGTATCGTGATTATCAATTCA(AGAA)
2972_ORF_38_C_b	ACATATCGACGTATCGTGATTATCCCATTCA(TGAA)
2972_ORF_38_C_c	ACATATCGACGTATCGTGATTATCCCCTTCA(AGAA)
2972_ORF_38_C_e	ACATATCGACGTATCGTGATTATGCCATTCA(AGAA)
2972_ORF_44_WT	AGCCTAGATAGCGAAGTTGATCGTATCTATTT(AGAA)
2972_ORF_44_b	AGCCTAGATAGCGAAGTTGATCGTATCTGTTT(AGAA)

539 **G. Measure of phages fitness: determination of phage**  
540 **proportion during the competition experiment**

541 The qPCR mix was composed of 3  $\mu$ L of 2X Master Mix, 0.3  $\mu$ L of primers at 10  $\mu$ M,  
542 1.7  $\mu$ l of water and 1  $\mu$ l of phages solution at  $10^5$  or  $10^6$  PFU/mL. To specifically  
543 target the referee phage (ie the phage with a 37-bp deletion), we used primers 5'-  
544 TAGACCATGCGCAGAAGGGA-3' and 5'-CCACGATTTCAACGATACGC-3'. To  
545 amplify all phages, we used 5'-GAAAATCAGCAGCAAATGGC-3' and 5'-TGACCA-  
546 CATCTTCTAAGCCGT-3'. The qPCR program was as follows: an initial denaturation  
547 at 95°C for 10 minutes, 45 amplification cycles of 15 seconds at 95°C, 20 seconds at  
548 58°C, 25 seconds at 72°C. To obtain melting curves, temperature reached 95°C for 5  
549 seconds, 60°C for a minute and rose to 97°C at a rate of 0.11°C per second. The DNA  
550 was cooled down at 40°C for 30 seconds. Calibration curve was obtained by applying  
551 this protocol to known-phage ten-times dilutions from  $10^7$  PFU/mL to  $10^3$  PFU/mL.  
552 To attribute an absolute number of phages to each qPCR point, these dilutions were  
553 titrated simultaneously (see above).

554

555 In our collection, the Reference phage is targeted by the BIM that target *orf24* and  
556 carries a 37 bp deletion in its protospacer.

## H. Durability of CRISPR resistances

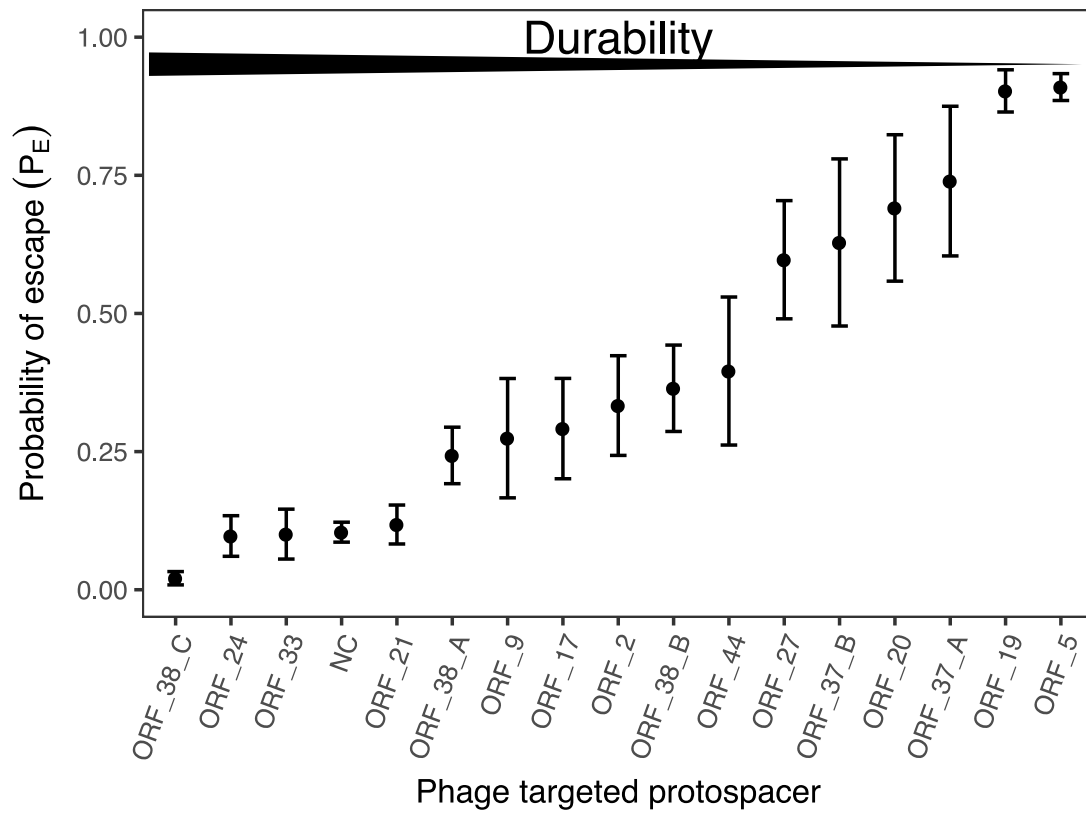


Figure S1: **Variability in the durability of CRISPR–Cas immunity.**

The probability of escape  $P_E$  was measured for each BIM using fluctuation tests. Mutation rates of each protospacer can be found in supplementary information I.

## I. Mutation rate of CRISPR-targeted sequences

Table S6: Mutation rate and 95% Confidence Intervals of phage protospacers. Mutation rates were measured using fluctuation tests (see Materials and Methods).

Name	Mutation rate	95% Confidence Interval
NC	$4.9 \times 10^{-8}$	$[3.1 \times 10^{-8}, 6.7 \times 10^{-8}]$
ORF_2	$1.9 \times 10^{-7}$	$[6.8 \times 10^{-8}, 3.1 \times 10^{-7}]$
ORF_5	$1.1 \times 10^{-6}$	$[8.6 \times 10^{-7}, 1.3 \times 10^{-6}]$
ORF_9	$1.5 \times 10^{-7}$	$[2.7 \times 10^{-8}, 2.8 \times 10^{-7}]$
ORF_17	$1.6 \times 10^{-7}$	$[4.5 \times 10^{-8}, 2.8 \times 10^{-7}]$
ORF_19	$1.2 \times 10^{-6}$	$[6.2 \times 10^{-7}, 1.7 \times 10^{-6}]$
ORF_20	$6 \times 10^{-7}$	$[2.5 \times 10^{-7}, 9.5 \times 10^{-7}]$
ORF_21	$5.7 \times 10^{-8}$	$[2.1 \times 10^{-8}, 9.2 \times 10^{-8}]$
ORF_24	$4.6 \times 10^{-8}$	$[1.0 \times 10^{-8}, 8.2 \times 10^{-8}]$
ORF_27	$4.3 \times 10^{-7}$	$[2.2 \times 10^{-7}, 6.5 \times 10^{-7}]$
ORF_33	$4.8 \times 10^{-8}$	$[4.6 \times 10^{-9}, 9.2 \times 10^{-8}]$
ORF_37_A	$7.1 \times 10^{-7}$	$[2.9 \times 10^{-7}, 1.1 \times 10^{-6}]$
ORF_37_B	$5.1 \times 10^{-7}$	$[1.6 \times 10^{-7}, 8.6 \times 10^{-7}]$
ORF_38_A	$1.3 \times 10^{-7}$	$[6.5 \times 10^{-8}, 1.9 \times 10^{-7}]$
ORF_38_B	$2.1 \times 10^{-7}$	$[9.3 \times 10^{-8}, 1.3 \times 10^{-7}]$
ORF_38_C	$9.4 \times 10^{-9}$	$[-1.2 \times 10^{-9}, 2.0 \times 10^{-8}]$
ORF_44	$2.5 \times 10^{-7}$	$[5.2 \times 10^{-8}, 4.4 \times 10^{-7}]$

559 **J. Mutation profile of escape phages**

Table S7: Profile of substitutions carried by phage escape mutants. 27 substitutions are transversions and 16 are transitions.

Type of substitution	Substitution	Number of occurrences
Purine Transition	A → G	6
	G → A	6
Pyrimidine Transition	C → T	1
	T → C	3
Transversion	A → C	4
	C → A	4
	A → T	7
	T → A	1
	T → G	0
	G → T	8
	G → C	1
	C → G	2

560 **K. Escape phage relative fitness**

561

Table S8: Relative fitness of escape phages. Deleterious mutations are highlighted in dark grey and neutral mutation in medium grey.

Phage escape mutants	Relative Fitness
2972_NC_a	0.688
2972_NC_c	-2.135
2972_NC_d	-2.072
2972_NC_e	-2.590
2972_ORF_2_a	-3.086
2972_ORF_2_b	-1.573
2972_ORF_2_c	-0.754
2972_ORF_5_a	-5.005
2972_ORF_9_a	-1.134
2972_ORF_9_b	-1.056
2972_ORF_17_a	-1.462
2972_ORF_17_b	-3.013
2972_ORF_17_d	-3.864
2972_ORF_19_a	-2.424
2972_ORF_19_b	-4.333
2972_ORF_20_b	-2.959
2972_ORF_21_a	-4.134
2972_ORF_21_c	-4.431
2972_ORF_21_d	-2.401
2972_ORF_24_c	-3.074
2972_ORF_27_a	-0.093
2972_ORF_27_d	-0.890
2972_ORF_33_a	-2.861
2972_ORF_33_b	-0.426
2972_ORF_33_c	-0.657
2972_ORF_37_A_a	-0.840
2972_ORF_37_B_a	-5.290
2972_ORF_37_B_b	0.458

Continued on next page.

Phage escape mutants	Relative Fitness
2972_ORF_37_B_c	-2.365
2972_ORF_37_B_d	-1.940
2972_ORF_38_A_a	-4.355
2972_ORF_38_A_b	-1.311
2972_ORF_38_A_e	-1.652
2972_ORF_38_B_a	0.415
2972_ORF_38_B_c	-4.282
2972_ORF_38_C_a	-3.166
2972_ORF_38_C_b	-6.212
2972_ORF_38_C_c	-2.674
2972_ORF_38_C_e	-0.215
2972_ORF_44_b	0.150



563 **L. Impact of synonymous mutations on the fitness of phage**  
564 **escape mutants**

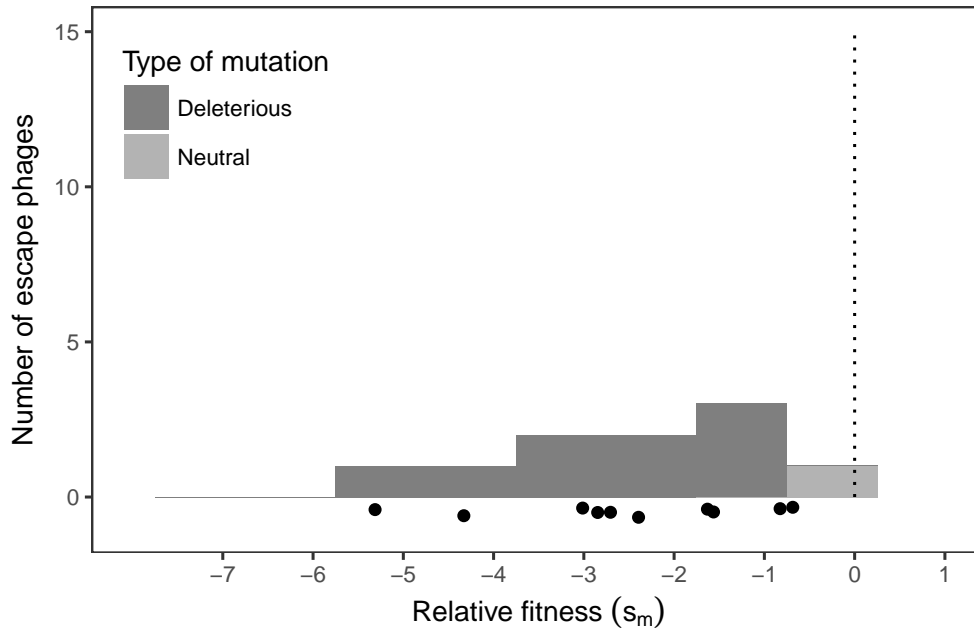


Figure S2: **Distribution of fitness effects of synonymous escape mutations in the phage.**

Relative fitness was measured through competition experiments with a collection of 10 escape phages with a synonymous mutation on their seed or PAM sequences. Phages that carry a neutral and deleterious mutations are represented in medium and dark grey respectively. Black dots show the relative fitness of each escape phage. The dotted segment represents the fitness of WT phage 2972. Fitness value of each escape phage is also provided in the supplementary informations K.

565